Chapter 3
Twenty-Three Kilometres of Superfluid Helium Cryostats for the Superconducting Magnets of the Large Hadron Collider (LHC)

Philippe Lebrun

Abstract The Large Hadron Collider (LHC) at CERN is the world's largest scientific instrument. The 1600 "high-field" superconducting magnets that make up the 23 km circumference accelerator ring represent the largest use of superfluid helium (He II) to date. This chapter describes the design evolution of the LHC magnet cryostats with particular emphasis on the He II cooling system, thermal insulation system and structural supports. Prototype testing, series production, installation and commissioning of these cryostats is also discussed. Numerous figures and tables illustrate the cryostat and present performance results.

3.1 The LHC and Its Cryogenic System

The Large Hadron Collider (LHC) at CERN, the European Organization for Nuclear Research near Geneva, is the largest research instrument ever built, and the most advanced tool in elementary particle physics (Fig. 3.1): its two combined synchrotrons, 26.7 km in circumference, accelerate and bring into collision intense counter-rotating beams of protons and ions at high energy, to probe the structure of matter and study the forces of nature at the unprecedented scale of tera-electron-volt (TeV) per elementary constituent [1]. This energy, about thousand times the mass of the proton, corresponds to the temperature conditions in the early universe 10^{-10} s after the Big Bang: the LHC therefore constitutes a powerful time machine, in particular to explore the mechanism of electro-weak symmetry breaking which occurred in the very early universe and to search for possible constituents of dark matter, relics from this period. In terms of length scale, 1 TeV is equivalent to 10^{-18} m, and the LHC may thus also be seen as an ultra-microscope resolving dimensions thousand times smaller than the proton. Exploration of this *terra incognita* has already led to the discovery of the long-sought Higgs boson in 2012,

P. Lebrun (✉)
CERN, European Organization for Nuclear Research, Geneva, Switzerland
e-mail: Philippe.Lebrun@cern.ch

J.G. Weisend II (ed.), *Cryostat Design*, International Cryogenics Monograph Series,
DOI 10.1007/978-3-319-31150-0_3

Fig. 3.1 Outline of the Large Hadron Collider in the Geneva area (CERN photo)

and is continuing with precision measurement of its properties as well as with search for new physics, "beyond the Standard Model".

To guide and focus its rigid beams along the accelerator tunnel, the LHC uses more than 1600 high-field superconducting magnets operating in 80 t of superfluid helium at 1.9 K (Fig. 3.2). In addition to enhancing the performance of the Nb-Ti superconductor by lower temperature operation, the LHC magnet cooling scheme exploits the unique thermo-physical properties of superfluid helium for stabilization against thermal disturbances and for heat transport. The superconducting magnets operate in baths of "pressurized" helium II—i.e. above saturation pressure, in fact sub-cooled liquid—close to atmospheric pressure. The large, but finite thermal conductivity of helium II for heat fluxes of technical interest ensures that each bath is quasi-isothermal, but is however insufficient to transport heat over long distances in the accelerator tunnel. The 106.9 m long magnet strings are therefore cooled via a heat exchanger tube threading its way in the cold mass, inside which a small two-phase flow of saturated helium II gradually vaporizes as it absorbs heat from the pressurized helium II baths (Fig. 3.3). This efficient cooling scheme presents several benefits [2], among which those of avoiding the need for circulation pumps and of minimizing the need for flow space in the transverse cross-section of the magnet. The large size of the collider ring, and its implantation some 100 m underground, limiting access to eight points around its perimeter, result in sector lengths of 3.3 km individually serviced as concerns accelerator and technical systems.

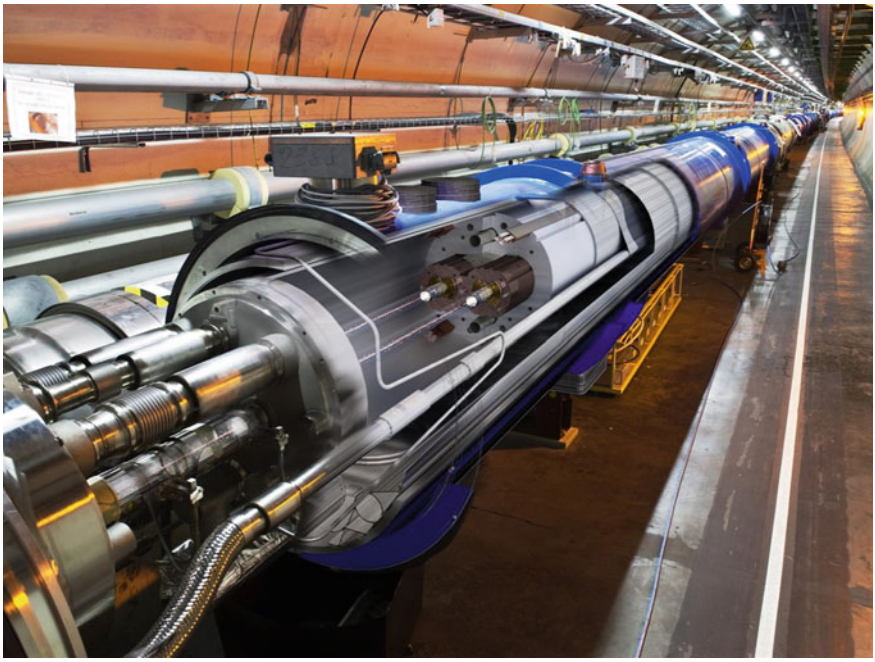

Fig. 3.2 The LHC cryomagnets installed in the tunnel (CERN photo)

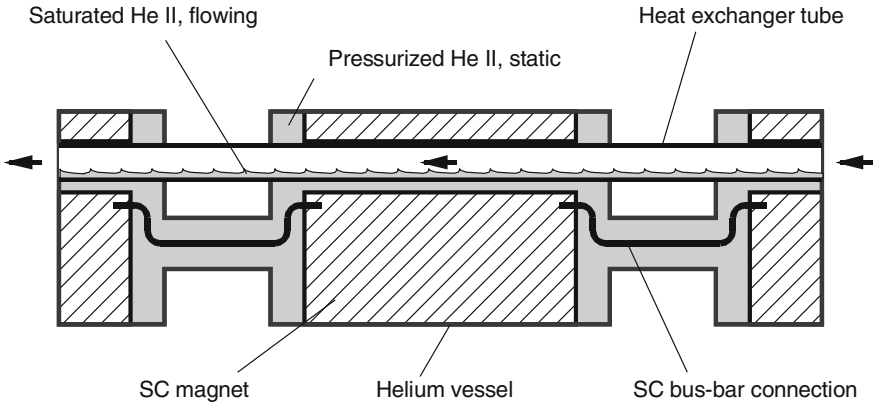

Fig. 3.3 Principle of the superfluid helium cooling scheme of the LHC magnets

The LHC ring is cooled by eight large-capacity cryogenic plants, each normally cooling a 3.3 km sector, but able to serve two adjacent sectors and thus provide redundancy at partial load. This requires distributing and recovering helium flows at different temperatures in the access shafts and along the machine tunnel over lengths of up to 3.3 km, by means of a compound cryogenic distribution line running along

the magnets and feeding each 106.9 m string in parallel. Each cryogenic plant provides a mix of liquefaction and refrigeration duties at 50–75 K and 4.5–20 K, amounting to an equivalent entropic capacity of 18 kW at 4.5 K. It is complemented at its cold end by a 1.8 K stage producing up to 2.4 kW of refrigeration power, by means of multi-stage sub-atmospheric compression using cold hydrodynamic and room-temperature volumetric compressors. Precooling the 37,500 t cold mass down to about 100 K is achieved by vaporization of some 10,000 t liquid nitrogen. Liquid nitrogen is otherwise not used in the system. 21,300 sensors monitor the machine cryogenics, while 4700 analog control loops ensure its operation. The cryogenic system of the LHC is described in Ref. [3].

In the following we tell the LHC cryostat story, approximately following chronological order, from the first studies and experimental work which enabled to establish the feasibility of such a large, novel superfluid helium system, to the several generations of prototypes meeting the evolution of machine configuration, their industrialization, series production and assembly, installation and interconnection in the tunnel, commissioning and operational experience. Focus is on the eight, 2818 m long continuous cold strings of the LHC arcs, containing in particular the 1232 dipole magnet cryostats (each 15 m in length) which constitute 85 % of the cold length and therefore drive the design, construction and industrialization choices, as well as the overall performance and cost of the system.

3.2 Feasibility of a Large Distributed Superfluid Helium System

The first approach to a large hadron collider to be installed in the existing tunnel housing the LEP collider, was based on twin-aperture dipole magnets using "cos θ" coils made of Nb_3Sn superconductor operated in baths of normal helium at 4.5 K, to produce a bending field around 10 T [4]. The study included the conceptual design of the corresponding cryogenic system, including cryostat simplified cross-section. It identified the main requirements and boundary conditions of large-capacity refrigerators at 4.5 K, thermal shielding at around 80 K, cryogenic fluid distribution along the 3.3 km sectors, cryogen storage, cooldown of the large magnet mass, quench handling and recovery and underground safety.

Soon after this it became clear that, in view of the limited availability, high cost and technical difficulty of implementing Nb_3Sn superconductors in accelerator magnets, the alternative of operating the more conventional Nb-Ti superconducting alloy at lower temperature in superfluid helium—to boost its current-carrying capacity at high field—should also be explored. This technique, pioneered at CEA Grenoble and first applied to cool high-field magnets for condensed-matter physics (the Grenoble High-Field Magnet) and nuclear fusion research (the TORE SUPRA tokamak at CEA Cadarache) [5], had however never been applied to the magnets and distributed configuration of a large circular accelerator. It clearly appeared that

the prime feasibility issues to be investigated were the management of heat loads (and thus the design of a cryostat meeting the required thermal performance) and the cryogenic distribution scheme—the latter also impacting the cryostat design to incorporate the cryogenic pipelines. A preliminary study of a superfluid helium cryogenic system for the LHC was then conducted [6].

A novel feature of the LHC with respect to previous superconducting accelerators is that the "static" heat loads, i.e. the heat in-leaks to the cold mass and other cryogenic components of the machine, represent only a fraction of the total. The large excitation currents of the magnets—12 kA for the LHC dipoles—induce resistive heating in the numerous non-superconducting joints between the winding layers, between the coils and between the magnets in a string: this additional "dynamic" heat load necessarily ends up into the helium bath at the lowest temperature level and must therefore be contained by a tight specification on the maximum joint resistance (typically lower than 1 nΩ per joint). Moreover, the circulation of intense particle beams in the accelerator rings also induces dynamic heat loads, through several processes such as dissipation of beam image currents in the resistive wall of the beam pipes, synchrotron radiation from the beams (in the UV range for LHC protons) and particle losses from the beam halo. While the latter produce cascades of secondary particles eventually depositing their energy into the magnet cold mass, the power of the other two processes may be intercepted at higher temperature in order to reduce its thermodynamic impact on the refrigeration system. This is the primary function devoted to the beam screens, the concept of which was introduced for the first time in the study. Today, beam screens cooled by supercritical helium between 5 and 20 K equip the LHC magnets and limit the heat load to the 1.9 K level to acceptable values; they also perform several other essential functions [7], in particular that of a distributed cryopump maintaining a good level of dynamic vacuum in the beam pipes, and their elaborate design is therefore the optimized result of a complex process involving several domains of accelerator physics and technology (Fig. 3.4). Pre-design of the cryostat featuring a 90 K thermal shield, non-metallic supports of the cold mass with heat intercepts at 90 and 4.5 K, multilayer reflective insulation around the cold mass, and integrating cryogenic distribution pipelines, gave an estimated heat in-leak at 1.9 K of 0.15 W/m. Containing the dissipation in the resistive joints to 0.05 W/m and introducing the beam screens to intercept most of the beam-induced heat loads yielded a total steady-state budget of 0.2 W/m at 1.9 K, to be compared with 0.9 W/m at 4.5 K for a normal helium cryostat in absence of beam screen. The conclusion of this preliminary study was that a superfluid helium cryogenic system for the LHC, including magnet cryostat and distribution scheme, appeared possible, though more complex than one at normal helium temperature.

The following years saw the refinement of such studies, particularly concerning the cryogenic distribution scheme and the assessment of dynamic heat loads, but the cryostat design concept (Fig. 3.5) and estimated performance of 0.15 W/m at 1.9 K were essentially confirmed [8]. The addition of a complete shield at 5 K surrounding the cold mass allowed—in principle—to reduce the residual gas conduction to the cold mass and thus the dependence of total heat load on the quality of

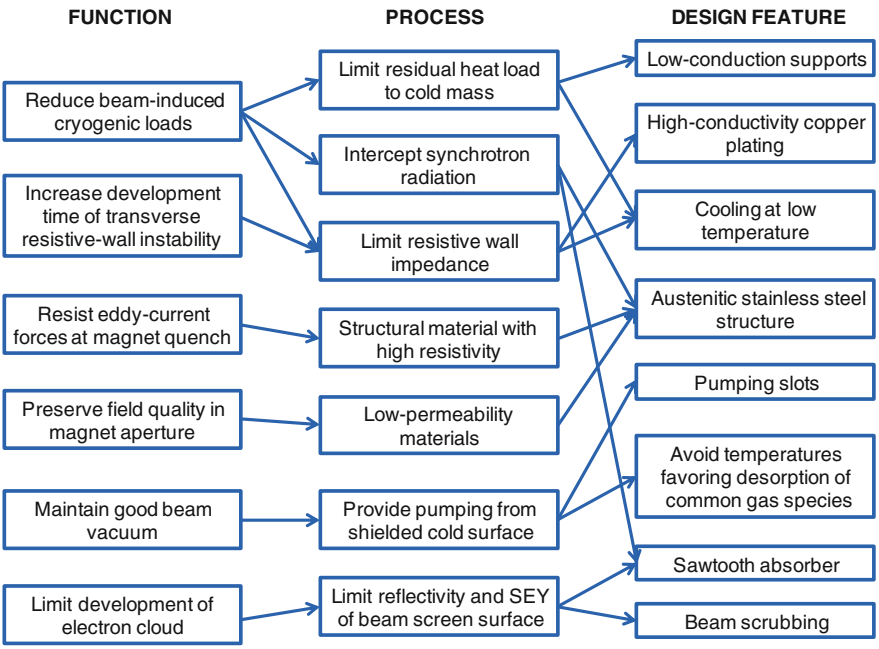

Fig. 3.4 Functional design map of beam screen for particle accelerator

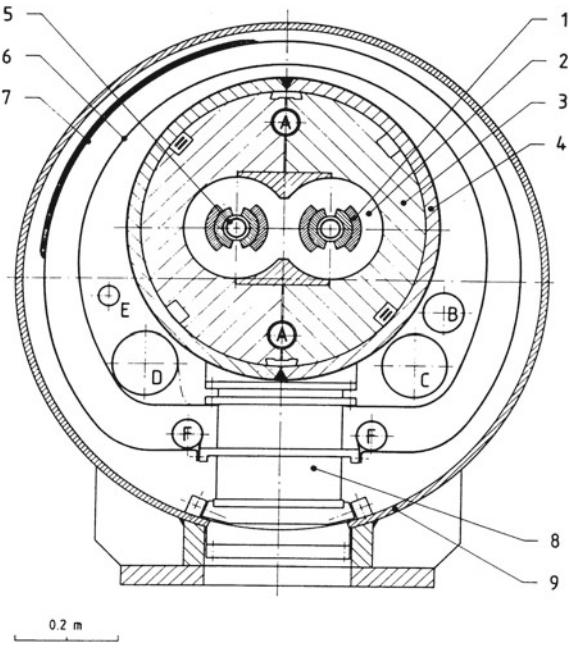

Fig. 3.5 Transverse cross-section of conceptual cryostat housing LHC twin-aperture dipole magnet at 1.9 K. *1* magnet coils; *2* magnet collars; *3* magnet yoke; *4* magnet shrinking cylinder and helium vessel; *5* beam screen; *6* shield at 5 K; *7* MLI insulated shield at 80 K; *8* non-metallic support post; *9* vacuum vessel; *A* helium II heat exchanger tube; *B–F* cryogenic distribution and recovery lines at 1.9, 5 and 80 K

the insulation vacuum. Assessment of the practical benefit of this additional feature led to several iterations discussed in the following.

The early conceptual studies of LHC cryostats benefitted, at least down to normal helium temperature, from the extensive design and development work performed in the USA, particularly at Fermi National Accelerator Laboratory in preparation for the SSC project [9]. Still, experimental validation of the LHC cryostat design proper was required, first by measurement of critical components and eventually on a full-scale prototype. A dedicated test set-up was built to perform precision heat in-leak measurements at 80, 4.2 and 1.8 K in the laboratory, combining several independent methods (cryogen boil-off, "heat-meters" i.e. calibrated thermal impedances, and transient temperature rise in a superfluid helium bath). Enabling the measurement of heat loads down to the mW range at 1.8 K, this experimental set-up was used *inter alia* to qualify support posts made of non-metallic composite materials (glass-fibre/epoxy and carbon-fibre/epoxy) and to optimize position and practical realization of their heat intercepts [10]. Another critical source of heat in-leak in the LHC cryostat stems from the 50,000 m^2 lateral surface area of the cold mass—the equivalent of seven soccer fields—receiving heat by radiation and residual gas conduction from the 80 K thermal shield in case a 5 K shield is not used or difficult to thermalize at its nominal temperature. It was therefore necessary to compare, on samples of practical geometry and size, the performance of several reflective single-layer and multilayer systems at low boundary temperature and in different conditions of insulation vacuum. This was done on a dedicated set-up housing a 3 m^2 cylindrical sample of the insulation system to be tested, with possibility of varying the warm and cold boundary temperatures [11]. It confirmed that very low heat fluxes can be achieved by passive, reflective systems in good vacuum, and that multilayer systems show a clear advantage to limit heat flux runaway in case of degraded insulation vacuum.

An opportunity to build rapidly a quasi-full-scale, twin-aperture prototype dipole was provided by the termination of series production of superconducting magnets for the HERA proton ring. Two sets of spare Nb-Ti dipole coils from the HERA production line were integrated into a common yoke to build a 9.15 m long twin-aperture prototype (TAP), to be operated in superfluid helium in order to simulate a LHC dipole: it was estimated that a field of 7.5 T could be produced with the coils powered at 8610 A. The TAP magnet needed a dedicated cryostat to be operated and tested in superfluid helium. Conversely, this provided a unique opportunity for experimenting, for the first time and almost in full scale, the design of the LHC cryostats and for studying some of the thermal and mechanical problems associated with their cryogenic operation.

The TAP cryostat [12] was designed at CERN along the principles of the conceptual LHC cryostats (Fig. 3.6) and built by industry. In addition to the magnet, it housed cryogenic distribution pipelines—some of which were used for heat interception—and featured three glassfibre/epoxy posts supporting the magnet, the central one fixed longitudinally and the other two allowed to follow the thermal contraction of the cold mass via rollers on tracks fitted to the vacuum vessel. These rollers and tracks were also used during assembly to insert the cold mass into the

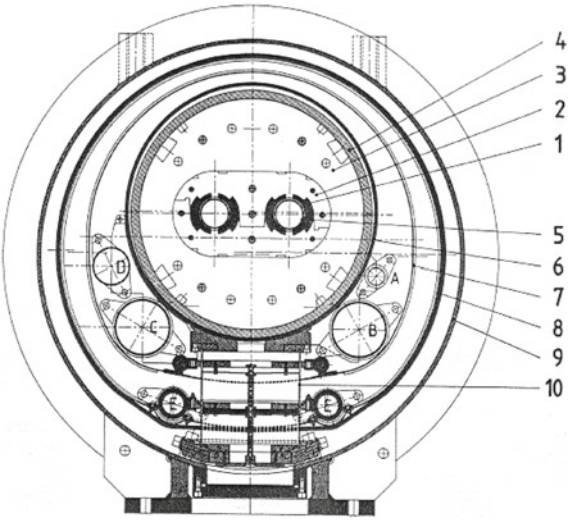

Fig. 3.6 Transverse cross-section of the TAP magnet and cryostat. *1* HERA-type superconducting coils; *2* magnet collars; *3* magnet yoke; *4* magnet shrinking cylinder; *5* cold bore tube; *6* helium vessel; *7* screen at 5 K; *8* thermal shield at 80 K with MLI; *9* vacuum vessel; *10* support post; *A & B* 1.8 K helium pipes; *C & D* 4.5 K helium pipes; *E* liquid nitrogen pipes

vacuum vessel. Demountable shipping restraints were provided to take transport acceleration loads. A liquid-nitrogen cooled thermal shield wrapped with 30 layers of MLI intercepted most of the radiative heat in-leak from room temperature, and a second screen surrounded the cold mass and pipeline assembly, actively cooled from 4.5 K pipes. The all-welded, austenitic stainless steel (AISI 304L) helium enclosure had a design pressure of 2 MPa to allow fast cooldown/warmup and resist resistive transitions of the magnet. The vacuum vessel was made of unalloyed construction steel (with austenitic stainless steel flanges), for reasons of magnetic shielding of the stray flux and cost in view of a large series production. Its inner surface was protected by low-outgassing epoxy paint compatible with high-vacuum operation. The cylindrical shell was provided with reinforcement rings at the longitudinal positions of the cold mass supports.

The TAP magnet was integrated into its cryostat by industry and shipped to CEA Saclay for cold tests. The magnet and cryostat performed very well, with maximum field of 8.25 T reached after seven resistive transitions, excellent leak-tightness of the superfluid helium enclosure, heat in-leak below 1 W at 1.8 K and about 4.6 W at 4.5 K [13]. Following resistive transitions of the magnet, high values of peak pressure, up to 3 MPa, were measured in the annular space between coils and cold bore tube at mid-length, thus raising concern about the choice of design pressure for the helium enclosure. A dedicated study based on a hydrodynamic model using thermo-physical properties of helium [14] confirmed the measurements and gave indications to limit this peak pressure, particularly when considering longer magnets. From the cryostat point of view, the TAP project established the soundness of the design principles and boundary conditions, confirmed performance expectations from design calculations and measurements on partial components and demonstrated the feasibility of industrial production at market price—including quality assurance, licencing procedures and operational safety.

3.3 Prototype Cryostats and String Tests

Based on the previous experience, a small series of cryostats were designed at CERN and procured from industry to house the first generation of 10 m long prototype dipole magnets, to be tested individually and later connected and operated in a string. The cryostats also had to accommodate the cryogenic distribution pipework sized for feeding a full LHC sector. Design requirements included heat in-leaks meeting the allowed thermal budget at the three temperature levels or ranges in the LHC cryogenic system (50–75 K, 4.5–20 K and 1.9 K), provision of a stable, precise and reproducible mechanical support for the magnet, withstanding of thermal and mechanical transients associated with rapid cooldown and magnet resistive transitions, as well as all possible failure modes. Technical solutions adapted to large series production were favoured.

The resulting design [15], inspired by the TAP cryostat but with a number of variants, is shown in Fig. 3.7. The cold mass support system still used three glassfibre/epoxy posts with two levels of heat interception, but the functions of assembly and of accommodation of longitudinal contractions were now handled separately, the former provided by a removable assembly trolley and the latter by sliding plates incorporating low-friction material. The support posts proper were developed and their construction optimized based on mechanical and thermal performance measurements [16]. The thermal shield at 80 K, made in commercially pure aluminium (AA 1100) to ensure good azimuthal temperature uniformity, consisted of a rigid lower tray incorporating a welded extruded aluminium profile providing the cooling channel, onto which a roughly cylindrical upper shell was tack-welded in four longitudinal sections. This compound construction provided sufficient mechanical rigidity and azimuthal thermal conduction to limit deflections of the shield during thermal transients, and thus avoid damage or thermal shorts.

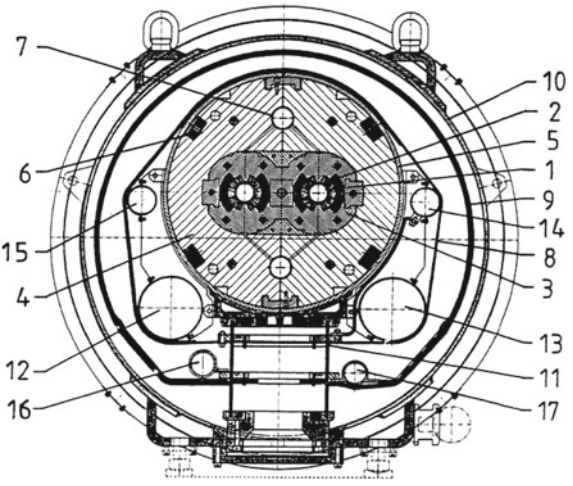

Fig. 3.7 Transverse cross-section of first-generation prototype dipole and cryostat. *1* cold bore; *2* magnet coils; *3* magnet collars; *4* magnet yoke; *5* magnet shrinking cylinder and helium vessel; *6* bus bars; *7* He II heat exchanger bore; *8* cold mass multilayer insulation; *9* thermal shield with multilayer insulation; *10* vacuum vessel; *11* support post; *12* 1.8 K GHe line; *13* 10 K GHe line; *14* 4.5 K He line; *15* 2.2 K LHe line; *16* 50 K GHe supply; *17* 70 K GHe return

The actively cooled 4.5 K screen surrounding the cold mass of the TAP cryostat was replaced here by a 10-layer blanket of MLI, partially thermalized onto the 4.5 K lines but insulated from the cold mass and 2 K lines by polyester spacers. Another, important novelty with respect to the TAP cryostat was the first engineering study and optimization of magnet and cryostat interconnection. To maximize the magnet filling factor of the machine and thus the beam energy reach, the interconnection space must be kept as short as possible, while allowing to reliably perform, inspect and test some 14 orbital welds joining 11 pipes. Space for automatic orbital welding and cutting machines, as well as for "clam shells" for local leak-testing of welds, was taken into account. The interconnection also includes all bellows accommodating construction and alignment tolerances, as well differential thermal contractions and displacements occurring in all possible phases of operation, including failure modes (as a reminder, the LHC cold mass shrinks by some 80 m in perimeter upon cooldown). Bellows specifications, including travel, misalignments, maximum rigidity and fatigue lifetime were established, pointing to hydro-formed multiply construction with external shells against buckling where needed. Samples were procured from several bellows manufacturers and extensively tested, thus providing a qualified industrial basis for future series procurement.

The design of the prototype dipole cryostat was adapted to house the main quadrupole, chromaticity sextupole and corrector magnets, beam position monitors and local cryogenic equipment as well as a vacuum barrier segmenting the insulation vacuum, all included in a so-called short-straight-section cryostat [17], and a prototype was built and tested.

In parallel with these activities, preparation was made to perform cryogenic tests of the magnets and cryostats. A 7200 m^2 test hall already equipped with a 6 kW at 4.5 K cryogenic refrigerator was further provided with a low-pressure helium pumping unit capable of 6 g/s at 1 kPa, upgradeable to 18 g/s with the addition of a cold booster compressor. Cooldown and warmup units, each providing up to 120 kW down to 100 K by vaporization of liquid nitrogen [18] were installed. The test station was planned to develop in a modular way following the ramp-up of series production, with up to twelve parallel test benches, the first two of which were commissioned to test prototypes [19]. Each bench, equipped with 18 kA current leads, could be operated independently of the others, only sharing—when and as much as needed—the common facilities such as normal liquid helium supply, pumping capacity at 1 kPa and gaseous helium flow for cooldown and warmup.

At the same time it was noted that precision thermal measurements on cryostats mounted on magnet test benches would be difficult to perform, due to parasitic heat loads (in particular the comparatively high heat in-leak coming from the anti-cryostats installed in the magnet apertures to perform magnetic measurements) as well as to schedule interference (reaching thermal steady-state requires long stabilization time incompatible with magnet turnaround on test benches). It was therefore decided to build a full-scale thermal model [20] from a 10 m prototype cryostat equipped with a dummy cold mass and finely instrumented. The cryostat

thermal model could be operated independently of the magnet tests station, allowing to vary parameters such as insulation vacuum and temperature levels, and providing precision of ±0.03 W at 1.8 K, ±0.1 W at 5–20 K and ±3 W at 50–75 K. Heat load measurements in nominal operating conditions on the thermal model showed excellent agreement with calculated values [21]. Moreover, several off-design runs enabled to measure the sensitivity of the cryostat heat in-leaks upon the temperature of heat intercepts and thermal shield, as well as on the residual pressure in the vacuum insulation space, also in good agreement with the calculations. The thermal performance of the prototype cryostats was therefore well understood in nominal and quasi-nominal conditions, and a mathematical model benchmarked on the experimental measurements could be used reliably to quantitatively assess its degradation in off-design conditions [22]. The pending question of the inner screen surrounding the cold mass, either "floating" or tentatively thermalized on the 5 K line, was then revisited [23], using realistic values of impedance for the thermalization contacts and net-type insulating spacers in MLI: the study indicated potential improvement for a thermalized system, from 60 mW/m^2 down to 30 mW/m^2 in good insulation vacuum (10^{-4} Pa), at the cost of increased complexity in cryostat assembly.

Another pending issue was that of using normal construction steel for the cryostat outer vessel, normally operating at room temperature but possibly subject to being cooled below the ductile-to-brittle transition temperature in case of catastrophic loss of insulation vacuum. This was tested on a full scale cryostat equipped with a dummy cold mass initially cooled at 80 K [24]. Upon breach of the vacuum with gaseous helium, heat transfer to the cold mass induced water condensation and frost formation on the outer vessel, but its minimum temperature reached at 260 K remained above the acceptable limit. Moreover, temperature evolution was slow enough to allow detection of the accident and implementation of remedial action, e.g. by bringing additional pumping speed to restore, at least partially, the insulation vacuum.

The prototype magnets in their cryostats were then assembled stepwise into a test string [25], a full-scale working model of the elementary cell of the machine lattice and local cryogenics, installed on a 1.4 % ramp corresponding to the maximum slope of the LHC tunnel, with a final length of 50 m [26]. The test string (Fig. 3.8) enabled us to practice assembly, leak-tightness and alignment procedures, then mechanical stability and vacuum measurements upon controlled cooldown of the 65-t cold mass, and finally cryogenic operation and control, magnet powering and discharge, handling of resistive transitions and recovery [27]. Vacuum and thermal transients were investigated, in particular as concerns non-standard operation and failure modes [28]. In spite of the absence of beam, the test string also served as an excellent training ground for young recruits, who eventually had to operate from a dedicated control room a compound system integrating several accelerator technologies, with many measurements and control loops. Finally, it constituted an important demonstrator which contributed to the approval of LHC construction by the CERN Council.

Fig. 3.8 First-generation LHC Test String (CERN photo)

In the last round of studies before project approval, several important changes were implemented in the configuration of the LHC and its cryogenic system. To minimize their number and the associated manufacturing and testing costs, the LHC dipole magnets had their length extended from the previous 10 m to the maximum

which could be practically transported in European roads (40-t limit) and conveniently handled for assembly, testing and installation, i.e. 15 m, thus requiring new, longer cryostats. In order not to lose in useful aperture, the cold mass had to be curved, with a horizontal sagitta of 9 mm, but the cryostats could remain straight. As concerns cryogenic system architecture, grouping all refrigeration equipment in the five points around the ring (instead of eight) already equipped with technical infrastructure led to significant cost savings, and allowed for redundancy at part-load, but cryogenic flows had then to be distributed over the full 3.3 km length of the sectors (instead of half-sectors). This required larger-diameter pipes which became difficult to integrate in the cryostat transverse cross-section. Consequently, all distribution pipework and local equipment was moved to a compound cryogenic line running in the tunnel along the magnets, and the remaining pipework in the cryostats was then limited to that needed for operation of the cryostat proper. Another important consequence is that the cryogenic line could be installed, commissioned and tested independently of the progress in magnet installation, thus bringing valuable schedule flexibility in the last phase of project construction [29]. Moreover, it had been observed that in view of the large size of the LHC ring, "passive" cryogenics, i.e. magnet cryostats and cryogenic distribution represented the largest share of the cost breakdown, in fact larger than "active" cryogenics, i.e. the refrigeration plants. Consequently, any simplification of the cryostats and cryogenic distribution scheme, even though it may result in increasing the refrigeration duty, would concur to lowering the total cost. A simplified cryogenic scheme was then implemented [30], with local cooling loops extending over the length of a full lattice cell (106.9 m) instead of the previous half-cell, implementation of local 4.5–2.2 K sub-cooling heat exchangers in each local cooling loop allowing the suppression of one pipe inside the distribution line, and a large overall reduction in the number of cryogenic components.

A second generation of prototype cryostats for dipoles [31] and short-straight-sections [32] was then designed and built, based on the experience acquired with the first-generation prototypes and incorporating the changes in LHC configuration described above. In the dipole cryostat (Fig. 3.9) the smaller outer diameter (914 mm) allowed the shell of the vacuum vessel to be made of standard, helically welded elements for pipelines, with a wall thickness of 12 mm. To prevent any risk of embrittlement, the construction steel used (DIN GS-21 Mn5) was however specified to have a minimum energy absorption of 28 J/cm^2 as measured in an ISO-standard Charpy test at 240 K. The shells were equipped with AISI 304L end flanges and reinforced, at the longitudinal positions of the magnet supports, by welded rings and forged brackets for lifting points and alignment fiducials. The longer, heavier cold mass was still supported on three posts, the longitudinal positions of which were compromised between minimizing vertical sagitta (Bessel conditions) and keeping the ends of the cold mass horizontal to ease interconnect assembly (Airy conditions). The vertical off-axis between magnet and cryostat axes was reduced to 80 mm, thus requiring shorter support post of 210 mm total height, redesigned to take higher combined loading of 125 kN in axial compression and 40 kN in shear [33]. The longer thermal shield, a quasi-cylinder cooled from one

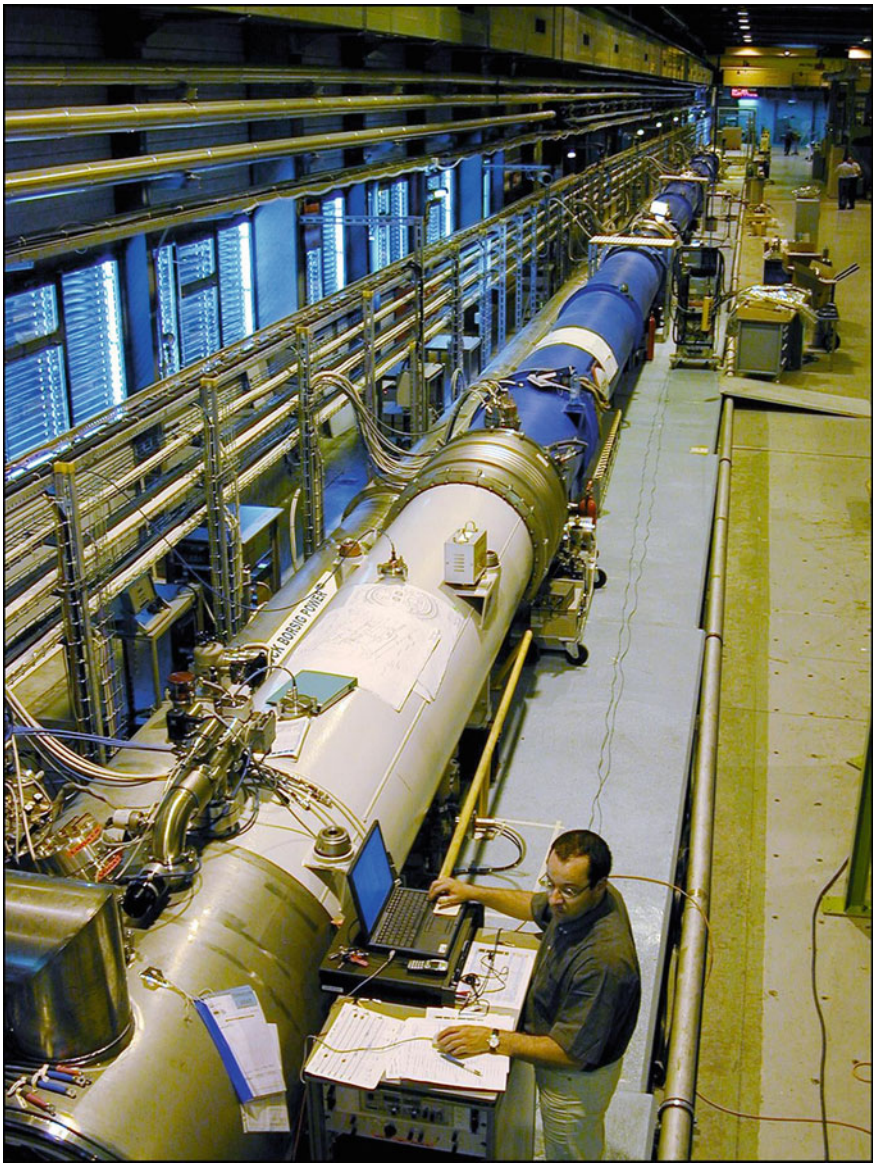

Fig. 3.9 Second-generation prototype cryostats assembled into second Test String (CERN photo)

generatrix, was prone to larger deformations upon thermal transients, with the risk of damage and unwanted thermal shorts [34]. The technical solution experimented in the first-generation prototypes, i.e. separating the functions of mechanical rigidity and azimuthal temperature homogeneity, was further refined towards industrialization: the lower tray was made of a full-length extrusion of A6060 aluminium

Fig. 3.10 Extruded aluminium alloy (A6060) bottom tray of cryostat thermal shield (CERN photo)

alloy, integrating two 80 mm diameter channels, one used for the cooling, the other left open (Fig. 3.10). The cooling channel was fitted at the ends with aluminium-to-stainless steel pipe transitions for interconnection. The upper shell of the thermal shield made of commercially pure aluminium A1100, was segmented in five sections (Fig. 3.11). A semi-rigid screen, thermalized to the 5 K pipes providing heat intercepts on the support posts was tentatively re-introduced in these cryostats with the aim of further reducing the heat in-leak on the cold mass. The cryostat interconnect was also redesigned to accommodate installation misalignments of up to ±4 mm in any direction and thermal contractions of up to 48 mm between the longitudinally fixed central posts of neighbouring dipoles. The short-straight section cryostat (Fig. 3.12), designed in collaboration with IPN Orsay (France) incorporated many design features of the dipole cryostat, and showed a similar transverse cross-section. It was equipped with a vacuum barrier for segmenting the insulation vacuum, and a cryogenic service module connected to the cryogenic distribution line by a multi-pipe "jumper" connection. The service module also contained beam position monitors, conduction-cooled current leads for the independently-powered orbit corrector magnets, and instrumentation feedthroughs. However, all local cryogenic equipment was now moved to the cryogenic line on the other side of the jumper connection.

Fig. 3.11 Aluminium A1100 shell of cryostat thermal shield (CERN photo)

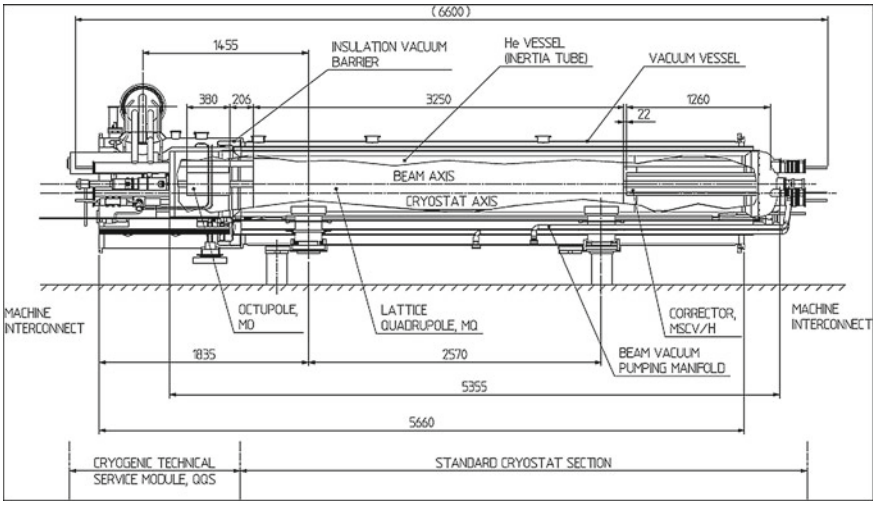

Fig. 3.12 Longitudinal cross-section of the second-generation short-straight-section cryostat

Five second-generation dipole cryostats, and two short-straight section cryostats were procured from industry and assembled around their magnets for cold testing and installation into a 107 m long second-generation test string [35], the last large-scale experimental validation of the LHC accelerator systems before entering construction. A first systematic risk analysis of the LHC cryogenic system [36] established all possible failure modes and analysed their consequences, thus confirming the cryostat design parameters and safety features.

3.4 Industrial Series Production, Installation and Commissioning

The design of the series cryostats (Fig. 3.13) derived directly from the second-generation prototypes, the measured thermal performance of which was used to establish reliably a reference thermal budget for the purpose of sizing the cryogenic refrigeration plants and distribution system. A "heat-load working group" involving all stakeholders was established to collect all calculated and measured data, validate the estimates (Table 3.1) and track possible future evolutions.

Changes of a few manufacturing aspects streamlined the design towards industrialization in view of series production [37]. Trading moderate improvement

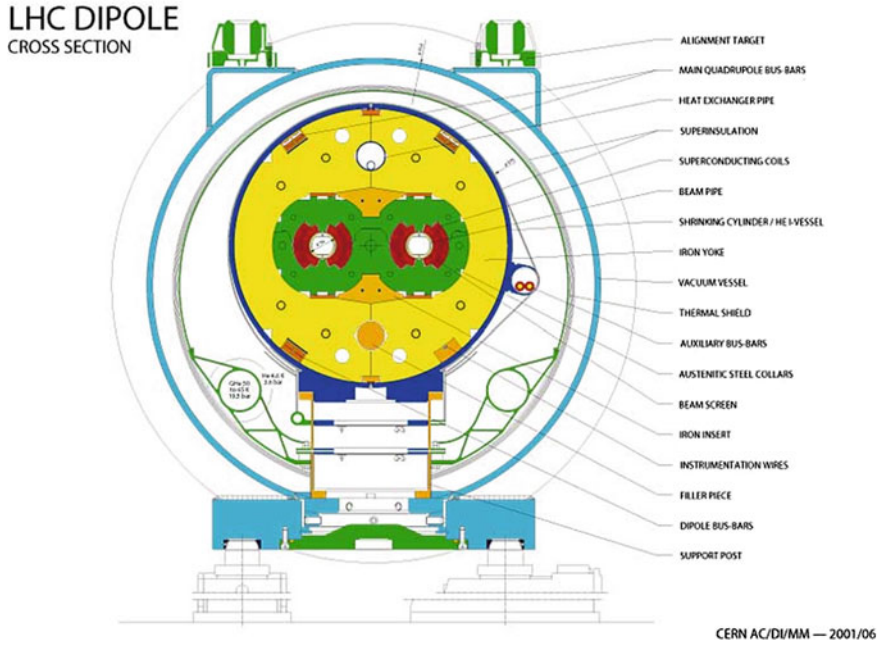

Fig. 3.13 Transverse cross-section of series dipole cryostat

Table 3.1 Heat in-leaks of 106.9 m long standard cell (6 dipoles and 2 short straight sections)

	50–75 K	4.5–20 K	1.9 K
Magnet support posts (W)	157	9.78	1.07
Thermal shield (W)	301	–	–
Cold mass MLI (W)	–	0.85	11.3
Beam screen (W)	–	–	1.62
Instrumentation feedthrough (W)	–	–	4.25
Beam vacuum feedthrough (W)	2.40	–	0.42
Orbit corrector current leads (W)	10.4	2.44	0.53
Beam position monitor (W)	–	0.93	0.60
Cryogenic service module (W)	–	0.01	0.21
Vacuum barrier (W)	11.6	0.03	0.42
Total heat in-leak (W)	**482**	**14.0**	**20.4**
Average linear heat in-leak (W/m)	**4.51**	**0.13**	**0.19**

Fig. 3.14 Glassfibre-reinforced epoxy support post (CERN photo)

of thermal performance against complexity and cost, the 5 K thermalization of the screen was finally not retained, and the cold mass was eventually covered with a 10-layer blanket of MLI. The complete rationale for this choice is summarized in Ref. [38]. Following completion of welding work, the series vacuum vessels were stress-relieved by vibration to ensure mechanical stability over time. Instead of the previously used low-outgassing epoxy paint, their inner surface was sandblasted and simply cleaned to high-vacuum standards, with no other surface treatment. Magnet support posts (Fig. 3.14) were composed of monolithic 4 mm thick

columns of glass-fibre reinforced epoxy, manufactured by resin-transfer moulding, a highly automated technique ensuring low production cost and reproducible quality for series of 4700 units [39]. At the heat intercept locations, external flanges of aluminium alloy and internal stainless-steel reinforcement rings are glued to the columns. Aluminium anti-radiation disks and reflective coating on the lower, warmer section exposed to radiation from the room-temperature outer vessel, complete the assembly. The 30-layer MLI around the thermal shield and 10-layer MLI around the cold mass were made of pre-fabricated blankets of 6 mm thick PET film, double-aluminized with 400 Å, interleaved by a very low weight polyester spacer. The developed perimeter of each blanket was adjusted to compensate for their differential thermal contraction with the stainless-steel and aluminium shells supporting them. Besides more precise manufacturing, pre-fabrication enabled the multilayer insulation systems to be assembled by non-specialized personnel, using Velcro™ fasteners, and avoided installation errors, thus ensuring future thermal performance of the multilayer insulation systems in the LHC ring.

For series production, it was decided to get the cryostats assembled by industry on the CERN premises, with CERN procuring all components and providing the contractors with a build-to-print specification, the use of two assembly halls totalling some 10,000 m^2 floor space, lifting and transport facilities, heavy and specialized tooling, detailed procedures and quality management tools, as well as with initial training of the execution personnel on the pre-series units, co-assembled with CERN experts (Figs. 3.15 and 3.16). Assembly of the 1232 dipole and 474 short-straight-section cryostats spanned five years, representing some 850,000 h of work with personnel numbers—operators and technicians—peaking at 145 [40].

Fig. 3.15 Dipole cryostat assembly hall (CERN photo)

Fig. 3.16 Short-straight-section cryostat assembly hall (CERN photo)

Following assembly, each cryo-magnet was moved to the test hall using a specially designed vehicle used for both lifting and transport (Fig. 3.17), connected to one of the twelve test benches, pumped down, cooled down and cryogenically tested, with the magnet powered up to 10 % above nominal (Fig. 3.18). Magnetic measurements in cold conditions were only performed on a fraction of the production. After removal from the test bench each cryo-magnet was allocated a position in the ring based on test results, prepared for installation and lowered to the tunnel level via a large, elliptical shaft equipped with a 40-t gantry crane with a hook travel of 54 m. The major axis of 18 m of the elliptical shaft is able to accommodate the full assembled length of a cryo-dipole, with protection end covers, horizontally (Fig. 3.19).

Cryostat assembly and cryogenic tests followed the production rate of magnets in industry (Fig. 3.20), while installation in the tunnel started later and proceeded at a faster rate. As a consequence, a large buffer storage of assembled and tested cryo-magnets was available, enabling the optimization of their final installation positions in the accelerator tunnel in order to reduce dispersion in the magnetic and geometrical properties of assembled sectors. The cryo-magnets were stored in the open air for several months, with their ends capped and insulation space kept under dry nitrogen.

Fig. 3.17 Completed dipole cryo-magnet transported to test hall (CERN photo)

Fig. 3.18 Cryogenic tests of magnets at CERN (CERN photo)

Transport in the tunnel from the shaft to the installation position was done via an optically guided, electrically powered trolley at low velocity (3 km/h) to minimize inertial forces in view of the large masses transported. On location, the cryo-magnet weight was loaded to a transverse transfer platform, and then transferred onto its pre-positioned final support jacks (Fig. 3.21). Electrical magnet interconnections and hydraulic cryostat interconnections were then performed. This was done by

Fig. 3.19 Lowering of cryo-magnet to LHC tunnel via elliptical shaft (CERN photo)

industry in the framework of a build-to-print contract. CERN developed the methods, special tooling and quality assurance procedures to be used by the contractor, and provided initial training of its personnel [41]. Some 40,000 cryogenic pipe welds were reliably executed using automatic TIG orbital welders (Fig. 3.22). The inner part of a completed cryo-magnet interconnection, with the MLI blankets, thermal shield and outer vacuum sleeve removed, is shown in Fig. 3.23. The domed ends of the helium vessels, as well as the reflective multilayer insulation blankets covering the cold mass and the thermal shield, are clearly visible on either side of the interconnection.

Following global pressure and leak-tightness tests, each 3.3 km sector of the LHC was cooled down and powered. Total sector heat in-leaks (Fig. 3.24) were measured within the estimated values [42], a final validation of the quality of the design, construction and installation of the cryostats.

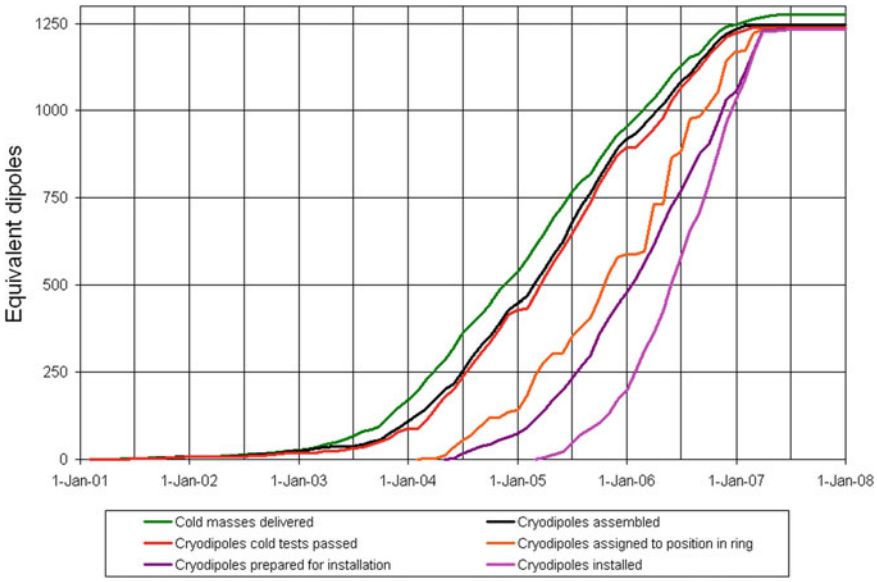

Fig. 3.20 Series production of LHC dipole cryo-magnets

Fig. 3.21 Transverse positioning of cryo-magnet on final location (CERN photo)

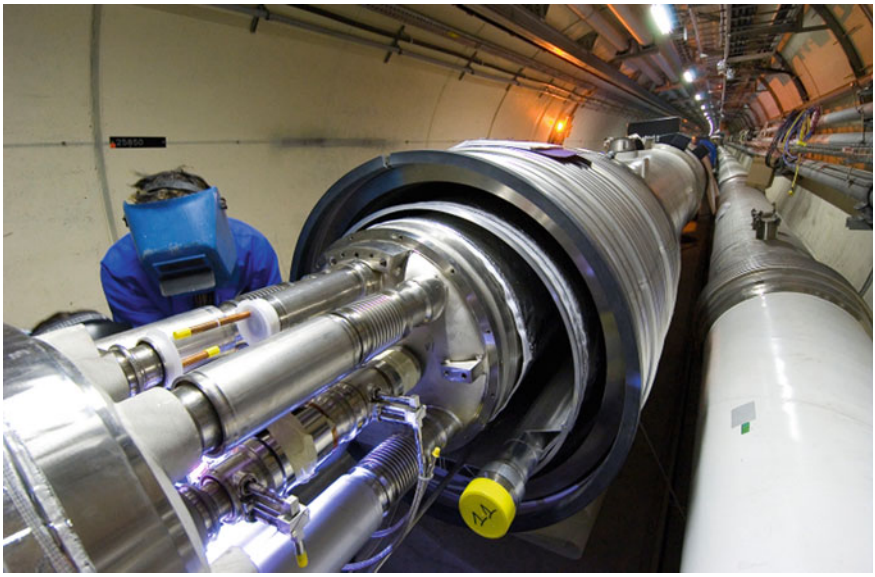

Fig. 3.22 Cryogenic piping interconnection in LHC tunnel by orbital TIG welding (CERN photo)

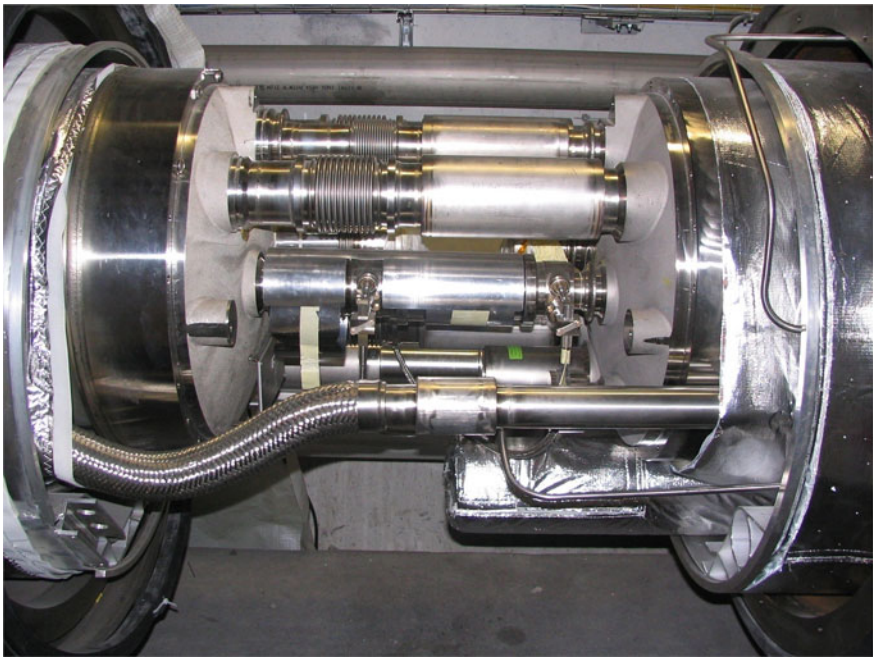

Fig. 3.23 Cryostat interconnection inner piping (CERN photo)

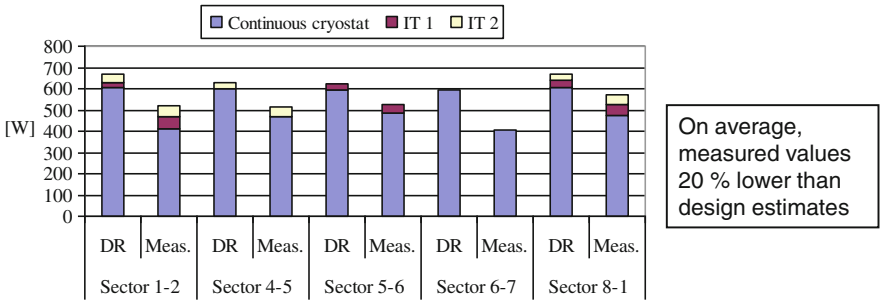

Fig. 3.24 Measured heat in-leaks of LHC sectors at 1.9 K (*DR* design report estimates; *IT* inner quadrupole triplet)

3.5 Concluding Remarks

The LHC contains the largest system of advanced, high-performance cryostats housing superconducting accelerator devices, and may thus be considered, *mutatis mutandis*, as reference for future, similar projects. Several lessons can be drawn from this experience.

The technology of superfluid helium can be reliably applied to very large systems built by industry. In particular, the design principles, construction techniques and quality assurance methods used in normal helium cryostats are fully adequate to ensure leak-tightness of superfluid helium enclosures.

Cryostats of superconducting accelerator devices, magnets or RF cavities, must meet complex and often conflicting geometrical, mechanical and thermal requirements, at the interface between accelerator physics and technology requirements, industrial manufacturing constraints and cost. Their design must therefore follow closely the changes in configuration of the project and sometimes drive them. It is therefore essential for the cryostat designers to be fully integrated with the project team and in close contact with the magnet, RF, cryogenics and vacuum groups.

Within the cryogenic system, the total cost of the cryostats and distribution lines often exceeds that of the refrigeration plants. Global optimization of the complete system is therefore necessary, which may lead to simplify cryostat construction at the cost of loss in thermal performance, rather than designing for lowest possible heat-in-leak.

The large amount of thorough design and development work performed at CERN and in partner laboratories on the LHC cryostats has contributed to significantly increase knowledge and confidence in the design, engineering and quality assurance methods for this type of equipment. It is interesting to note that this work has already found an application in another project. Cryostats similar to those of the LHC dipoles are housing the superconducting magnets of the beam line for the T2K long-baseline neutrino experiment at the J-PARC laboratory in Tokai, Japan [43]. On the training and education side, a tutorial on cryostat design inspired from the development of LHC cryostats was first prepared for the CERN Accelerator School

"Superconductivity and Cryogenics for Accelerators and Detectors" in 2002 [44] and is now part of the curriculum of the yearly European Course of Cryogenics commonly organized by the Technical University of Dresden, the Wroclaw University of Technology and the Norwegian University of Science and Technology Trondheim. This has been further developed as a course in a more recent venue of the CERN Accelerator School on "Superconductivity for Accelerators" [45].

Acknowledgments Having been involved in this work from the onset, the author has tried to convey his strong conviction that the success of LHC cryostats is the result of teamwork by many contributors at CERN, in partner laboratories and in industry. A number of them appear as co-authors in the reference list below. The expertise, dedication and hard work of all should be acknowledged.

References

1. LHC Design Report, vol. I, *The LHC Main Ring*, CERN-2004-003 (2004). ISBN 92-9083-224-0
2. P. Lebrun et al., Cooling strings of superconducting devices below 2 K: the helium II bayonet heat exchanger. Adv. Cryo. Eng. **43A**, 419–426 (1998)
3. P. Lebrun, Cryogenics for the Large Hadron Collider. IEEE Trans. Appl. Supercond. **10**, 1500–1506 (2000)
4. A. Asner et al., *A feasibility study of possible machine options*, in Proceedings of ECFA-CERN Workshop on Large Hadron Collider in the LEP Tunnel, Lausanne, CERN-84-10-V-1 (1984), pp. 49–142
5. G. Claudet, R. Aymar, Tore Supra and helium II cooling of large high-field magnets. Adv. Cryo. Eng. **35A**, 55–67 (1990)
6. G. Claudet et al., *Preliminary study of a superfluid helium cryogenic system for the Large Hadron Collider*, in Proceedings of Workshop on Superconducting Magnets and Cryogenics, Brookhaven BNL 52006 (1986), pp. 270–275
7. V. Baglin et al., *Cryogenic beam screens for high-energy particle accelerators*, in Proceedings of ICEC24-ICMC 2012 Fukuoka, Cryogenics and Superconductivity Society of Japan (2013), pp. 629–634
8. G. Claudet et al., *Conceptual study of the superfluid helium cryogenic system for the CERN Large Hadron Collider*, in Proceedings of ICEC12 Southampton, Butterworth (1988), pp. 497–504
9. T. Nicol, *SSC Collider Dipole Cryostat*, Chap. 2, this book
10. H. Danielsson et al., Precision heat inleak measurements on cryogenic components at 80 K, 4.2 K and 1.8 K. Cryogenics **32**(ICEC Supplement), 215–218 (1992)
11. P. Lebrun et al., Investigation and qualification of thermal insulation systems between 80 K and 4.2 K. Cryogenics **32**(ICMC Supplement), 44–47 (1992)
12. M. Granier et al., Design and construction of a superfluid-helium cryostat for a ten-meter long high-field superconducting dipole magnet. Cryogenics **30**(September Supplement), 98–102 (1990)
13. M. Granier et al., *Performance of the twin-aperture dipole for the CERN LHC*, in Proceedings of EPAC'92, JACoW (1992), pp. 1414–1416
14. P. Lebrun et al., Investigation of quench pressure transients in the LHC superconducting magnets. Cryogenics **34**(ICEC Supplement), 705–708 (1994)
15. J.-C. Brunet et al., Design of LHC prototype dipole cryostats. Cryogenics **32**(ICEC Supplement), 191–194 (1992)

16. M. Blin et al., Design, construction and performance of superconducting magnet support posts for the Large Hadron Collider. Adv. Cryo. Eng. **39A**, 671–678 (1994)
17. W. Cameron et al., Design and construction of a prototype superfluid helium cryostat for the Short Straight Sections of the CERN Large Hadron Collider. Adv. Cryo. Eng. **39**, 657–662 (1994)
18. V. Benda et al., Cryogenic infrastructure for superfluid helium testing of LHC prototype superconducting magnets. Adv. Cryo. Eng. **39**, 641–648 (1994)
19. V. Benda et al., Cryogenic benches for superfluid helium testing of full-scale prototype superconducting magnets for the CERN LHC project. Cryogenics **34**(ICEC Supplement), 733–736 (1994)
20. L. Dufay et al., A full-scale thermal model of a prototype dipole cryomagnet for the CERN LHC project. Cryogenics **34**(ICEC Supplement), 693–696 (1994)
21. V. Benda et al., Measurement and analysis of thermal performance of LHC prototype cryostats. Adv. Cryo. Eng. **41**, 785–792 (1996)
22. G. Riddone, *Theoretical Modelling and Experimental Investigation of the Thermal Performance of LHC Lattice Cryostats*. Doctoral Thesis, Politecnico di Torino (1996)
23. G. Ferlin et al., *Comparison of floating and thermalized multilayer insulation systems at low boundary temperature*, in Proceedings of ICEC16-ICMC 1996, North-Holland (1997), pp. 443–446
24. P. Lebrun et al., Experimental investigation of accidental loss of insulation vacuum in a LHC prototype dipole cryostat. Adv. Cryo. Eng. **41**, 799–804 (1996)
25. A. Bézaguet et al., The superfluid helium cryogenic system for the LHC test string: design, construction and first operation. Adv. Cryo. Eng. **41**, 777–784 (1996)
26. A. Bézaguet et al., *Cryogenic operation and testing of the extended LHC prototype magnet string*, in Proceedings of ICEC16-ICMC 1996, North-Holland (1997), pp. 91–94
27. M. Chorowski et al., Thermohydraulics of quenches and helium recovery in the LHC prototype magnet strings. Cryogenics **38**, 533–543 (1998)
28. P. Cruikshank et al., *Investigation of thermal and vacuum transients on the LHC prototype magnet string*, in Proceedings of ICEC16-ICMC 1996, North-Holland (1997), pp. 681–684
29. V. Benda et al., *Conceptual design of the cryogenic system for the Large Hadron Collider*, in Proceedings of EPAC'96 Sitges, JACoW (1996), pp. 361–363
30. M. Chorowski et al., A simplified cryogenic distribution scheme for the Large Hadron Collider. Adv. Cryo. Eng. **43A**, 395–402 (1998)
31. J.-C. Brunet et al., Design of the second-series 15 m LHC prototype dipole magnet cryostats. Adv. Cryo. Eng. **43A**, 435–441 (1998)
32. W. Cameron et al., The new superfluid helium cryostats for the Short Straight Sections of the CERN Large Hadron Collider. Adv. Cryo. Eng. **43A**, 411–418 (1998)
33. M. Mathieu et al., Supporting systems from 293 K to 1.9 K for the Large Hadron Collider. Adv. Cryo. Eng. **43A**, 427–434 (1998)
34. G. Peon, G. Riddone, L.R. Williams, *Analytical model to calculate the transient thermo-mechanical behaviour of long thin structures cooled from a pipe: application to the LHC dipole thermal shield*, in Proceedings of ICEC16-ICMC 1996, North-Holland (1997), pp. 477–480
35. E. Blanco et al., Experimental validation and operation of the LHC Test String 2 cryogenic system. Adv. Cryo. Eng. **49**, AIP Conf. Proc. **710**, 233–240 (2004)
36. M. Chorowski, P. Lebrun, G. Riddone, Preliminary risk analysis of the LHC cryogenic system. Adv. Cryo. Eng. **45B**, 1309–1316 (2000)
37. N. Bourcey et al., Final design and experimental validation of the thermal performance of the LHC lattice cryostats. Adv. Cryo. Eng. **49**, AIP Conf. Proc. **710**, 487–493 (2004)
38. P. Lebrun, V. Parma, L. Tavian, Does one need a 4.5 K screen in cryostats of superconducting accelerator devices operating in superfluid helium? Lessons from the LHC. Adv. Cryo. Eng. **59A**, AIP Conf. Proc. **1573**, 245–252 (2014)

39. V. Parma et al., The LHC cryomagnet supports in glass-fibre reinforced epoxy: a large-scale industrial production with high reproducibility in performance. Adv. Cryo. Eng. **54**, AIP Conf. Proc. **986**, 211–218 (2008)
40. A. Poncet, V. Parma, Series-produced helium II cryostats for the LHC magnets: technical choices, industrialization, costs. Adv. Cryo. Eng. **53A**, AIP Conf. Proc. **985**, 739–746 (2008)
41. J-Ph Tock et al., The interconnections of the LHC cryomagnets at CERN: strategy applied and first results of the industrialization process. IEEE Trans. Appl. Supercond. **18**(2), 116–120 (2008)
42. S. Claudet at al., *Cryogenic heat load and refrigeration capacity management at the Large Hadron Collider*, in Proceedings of ICEC22—ICMC 2008, KIASC (2009), pp. 835–840
43. T. Nakamoto et al., Construction of superconducting magnet system for the J-PARC neutrino beam line. IEEE Trans. Appl. Supercond. **20**(3), 208–213 (2010)
44. P. Lebrun, *Design of a cryostat for superconducting accelerator magnets: the LHC main dipole case*, in Proceedings of CAS Superconductivity and Cryogenics for Accelerator and Detectors, CERN-2004-008, ISBN 92-9083-230-4 (2004), pp. 348–362
45. V. Parma, *Cryostat design*, in Proceedings of CAS Superconductivity for Accelerators, CERN-2014-005 (2014), pp. 353–399. ISBN 978-92-9083-405-2